Supplementary Figures

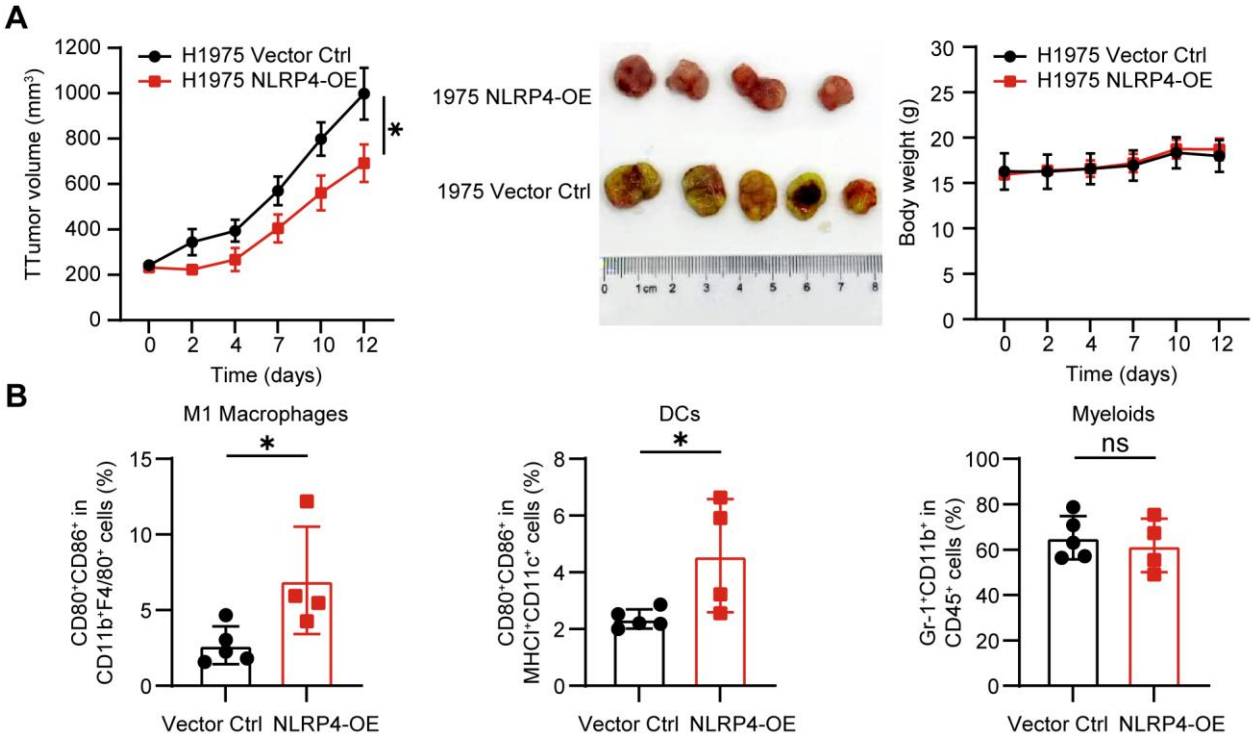

Figure S1 A Tumor growth curves, tumor volume at day 12, and body weight changes in BALB/c nude mice bearing H1975-Vector Ctrl or H1975-NLRP4-OE subcutaneous xenografts. Data were presented as mean ± SEM, analysed by two-way ANOVA. **B** Flow cytometric analysis of immune cell infiltration in subcutaneous tumors from H1975-Vector Ctrl and H1975-NLRP4-OE BALB/c nude mice. Data were presented as mean ± SD, analysed using two-tailed Student's t-test.

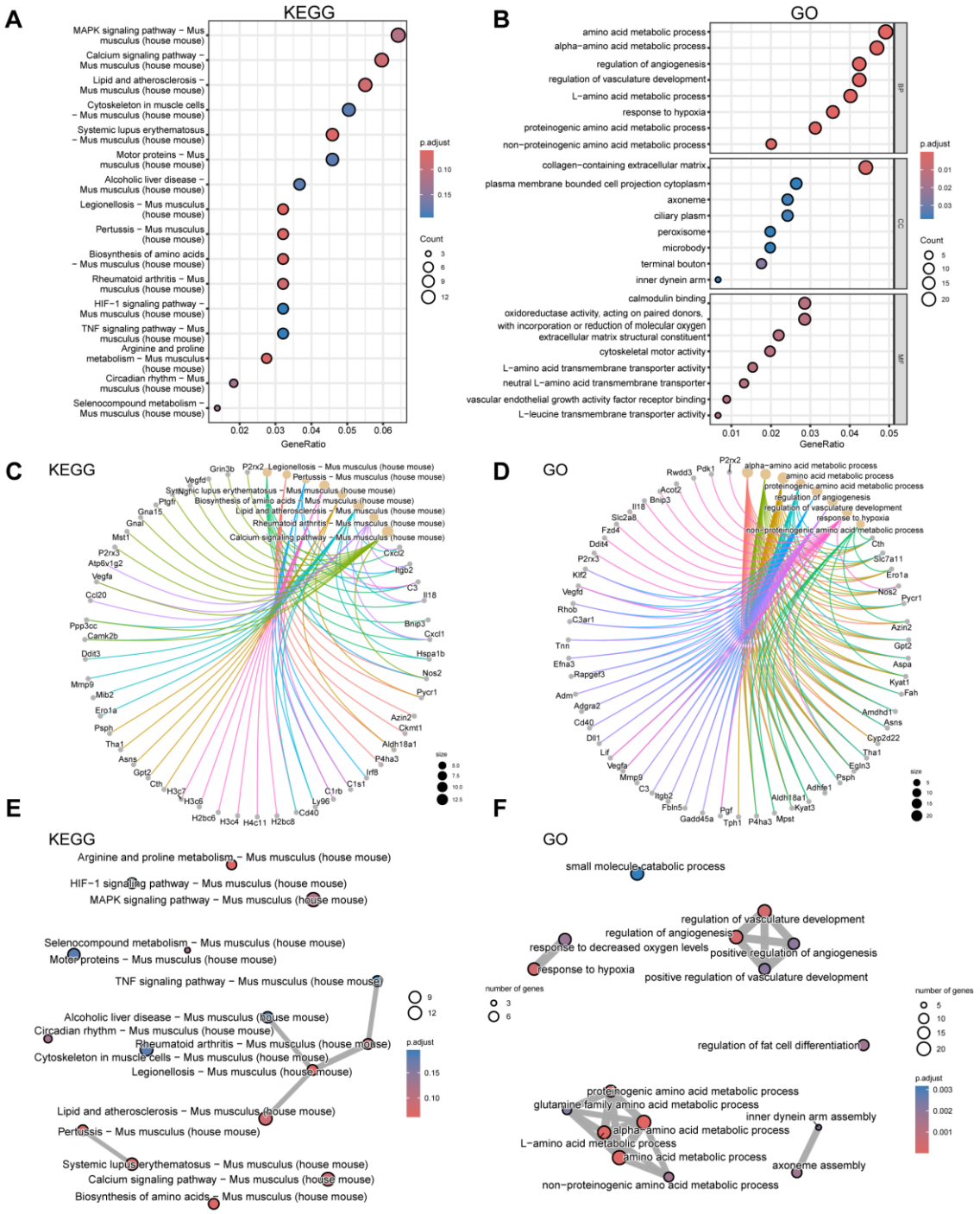

Figure S2 Functional enrichment analysis of differentially expressed genes between LLC-Nlrp4-OE and LLC-Vector Ctrl groups. A and B Bubble plots showed significantly enriched GO terms and KEGG pathways. Dot size represented the number of genes; color indicated the adjusted p-value. C and D Network plots visualized the connections between genes and the top-enriched GO/KEGG pathways. E and F Enrichment map illustrated the overlap and relationships among enriched GO terms and KEGG pathways.

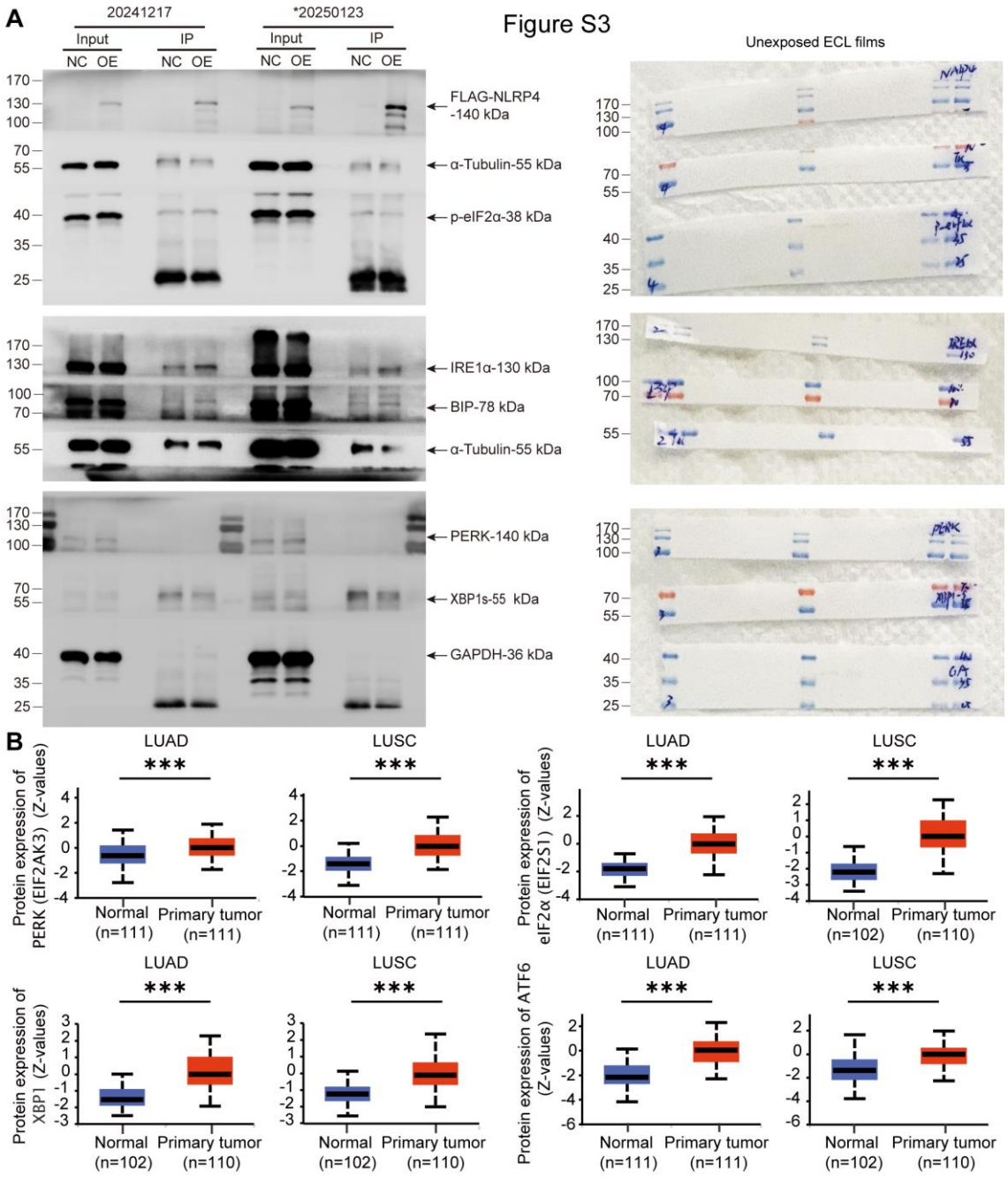

Figure S3 Original Western Blot Images and ER Stress Protein Expression Profiles. A Original Western blot images and corresponding unexposed ECL films from co-immunoprecipitation (Co-IP) assays of LLC-Vector control and LLC-NLRP4-OE cells. Data were shown from two independent sample collections (Experiment 1 and Experiment 2). Bands marked with an asterisk (*) correspond to the results presented in Figure 2B. B Bar chart showing relative expression of ER stress-related proteins in normal lung tissues and NSCLC patient samples. Data were presented as mean ± SD (bars) with individual data points (dots). Z-scores represented standard deviations from the median. Data were obtained from CPTAC and normalized within and across samples.

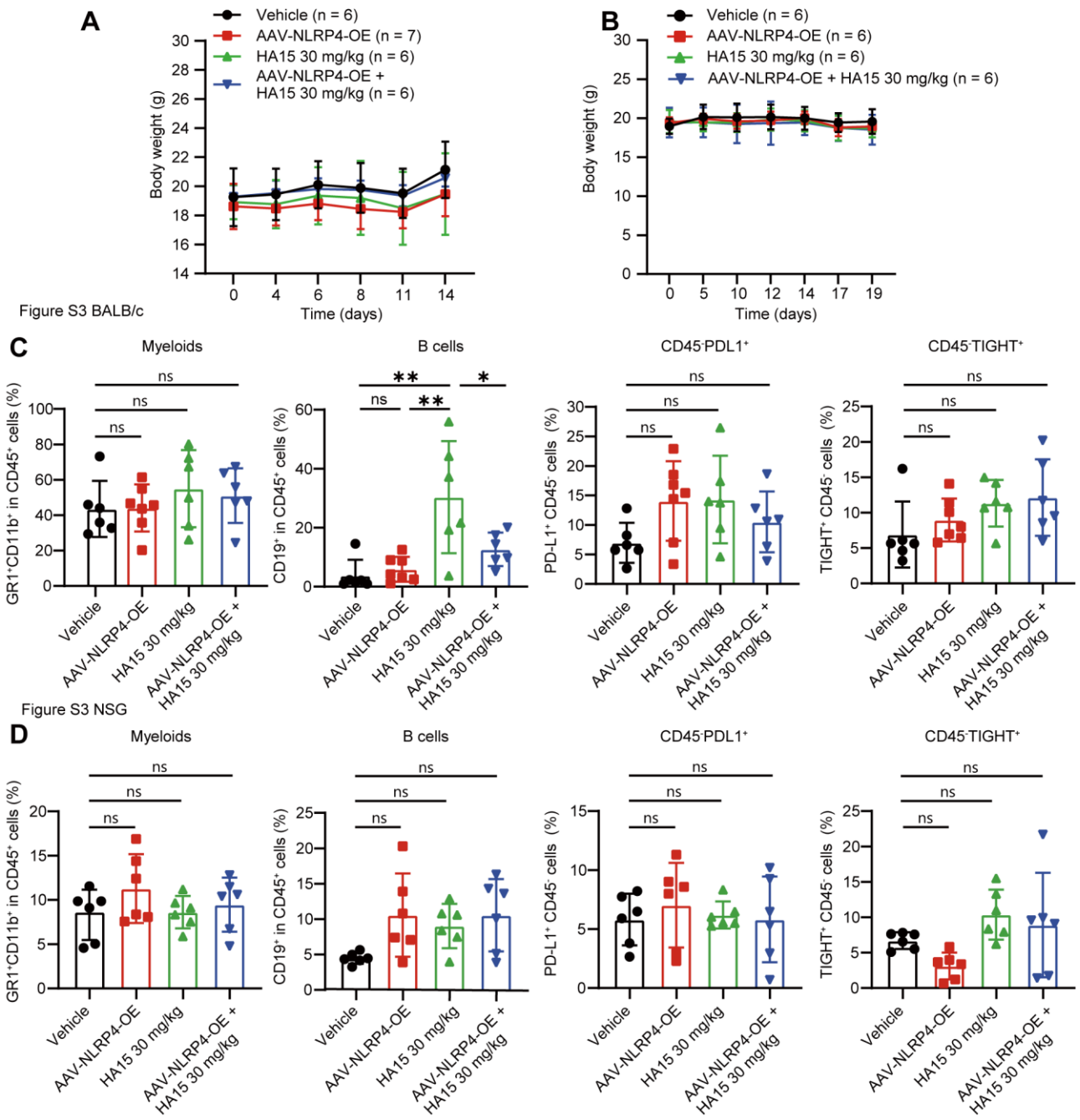

Figure S4 AAV-NLRP4 overexpression combined with a BIP inhibitor suppressed NSCLC tumor growth in BALB/c nude and NSG mice. A, B Body weight changes were monitored in mice bearing subcutaneous H1975-Vector control or H1975-NLRP4-OE tumors in BALB/c nude mice (A) and NSG mice (B). C, D Flow cytometric analysis of immune cell infiltration within the tumor microenvironment of subcutaneous tumors was performed in BALB/c nude mice (C) and NSG mice (D). Data were presented as mean ± SD, and statistical significance was determined using a two-tailed unpaired Student's t-test.

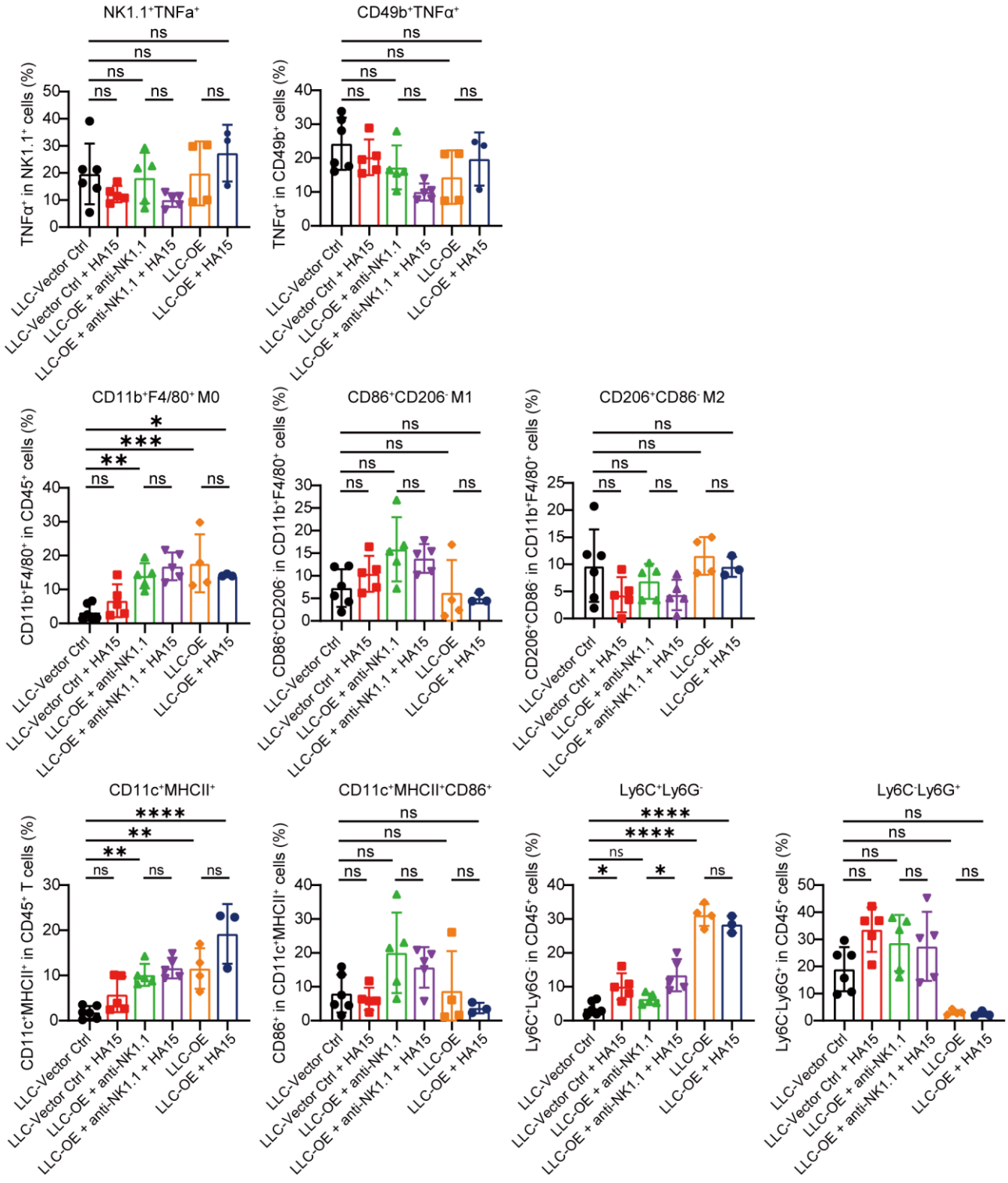

Figure S5 Flow cytometric analysis of tumor-infiltrating immune cells in C57BL/6J mice bearing LLC-Vector control or LLC-Nlrp4-OE tumors after NK cell depletion. Mice were treated with anti-NK1.1 to deplete NK cells, and the infiltration of immune cells in subcutaneous tumors was assessed by flow cytometry. Data were presented as mean ± SD and analyzed using a

two-tailed Student's t-test.

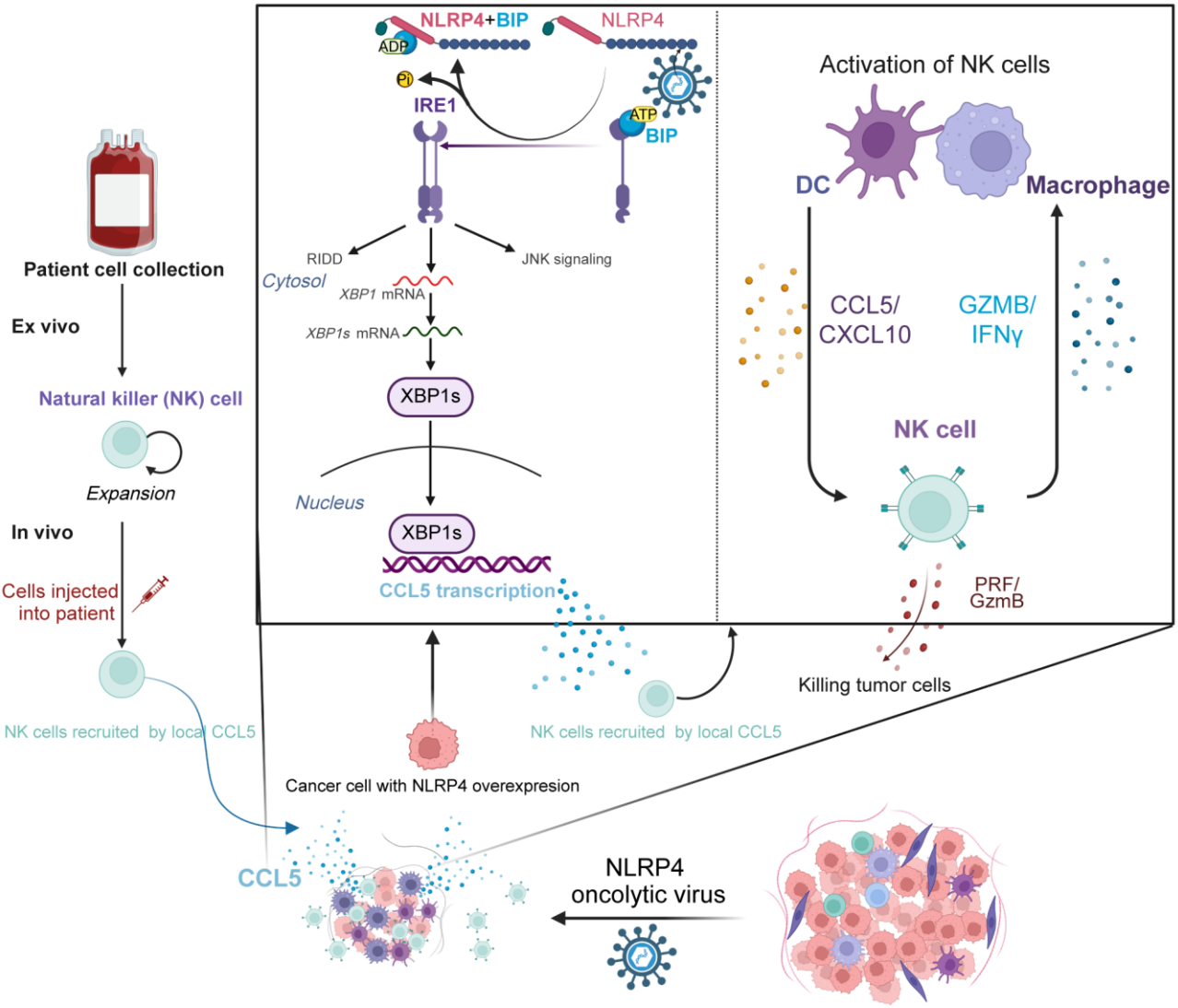

Figure S6. Proposed mechanism and therapeutic implications of NLRP4 in regulating NK cell function via ER stress. This process may establish a positive feedback loop, namely the NLRP4–ER stress–CCL5 axis, thereby enhancing anti-tumor immunity. The schematic model illustrating the origin of CCL5 and its potential application in CAR-NK therapy is informed by an independent ongoing study in our laboratory and highlights directions for future investigation.